Author Manuscript

Author Manuscript

Author Manuscript

Author Manuscript

HHS Public Access

Author manuscript

Neurobiol Aging. Author manuscript; available in PMC 2019 February 01.

Published in final edited form as:

Neurobiol Aging. 2018 February ; 62: 180–190. doi:10.1016/j.neurobiolaging.2017.10.014.

DNA damage and neurodegenerative phenotypes in aged *Ciz1* null mice

Mohammad Moshahid Khan, **Jianfeng Xiao**, **Damini Patel**, and **Mark S. LeDoux***

Departments of Neurology, and Anatomy and Neurobiology, University of Tennessee Health Science Center, Memphis, TN, 38163, USA

Abstract

Cell-cycle dysfunction and faulty DNA repair are closely intertwined pathobiological processes that may contribute to several neurodegenerative disorders. CDKN1A interacting zinc finger protein 1 (CIZ1) plays a critical role in DNA replication and cell-cycle progression at the G1/S checkpoint. Germline or somatic variants in *CIZ1* have been linked to several neural and extra-neural diseases. Recently, we showed that germline knock-out (KO) of *Ciz1* is associated with motor and hematological abnormalities in young adult mice. However, the effects of CIZ1 deficiency in much older mice may be more relevant to understanding age-related declines in cognitive and motor functioning and age-related neurological disorders such as isolated dystonia and Alzheimer disease. Mouse embryonic fibroblasts from $Ciz1^{-/-}$ mice showed abnormal sensitivity to the effects of γ-irradiation with persistent DNA breaks, aberrant cell-cycle progression, and apoptosis. Aged (18-mo-old) $Ciz1^{-/-}$ mice exhibited marked deficits in motor and cognitive functioning, and, in brain tissues, overt DNA damage, NF-κB upregulation, oxidative stress, vascular dysfunction, inflammation, and cell death. These findings indicate that the deleterious effects of CIZ1 deficiency become more pronounced with aging and suggest that defects of cell-cycle control and associated DNA repair pathways in post-mitotic neurons could contribute to global neurological decline in elderly human populations. Accordingly, the G1/S cell-cycle checkpoint and associated DNA repair pathways may be targets for the prevention and treatment of age-related neurodegenerative processes.

Keywords

cell cycle; CIZ1; DNA damage; aging; apoptosis

*Corresponding author, University of Tennessee Health Science Center, Department of Neurology, 855 Monroe Avenue, Suite 415 Link Building, Memphis, TN, 38163, USA, Telephone: 901-448-1662, mledoux@uthsc.edu.

Disclosure statement The authors declare no potential conflicts of interest.

Publisher's Disclaimer: This is a PDF file of an unedited manuscript that has been accepted for publication. As a service to our customers we are providing this early version of the manuscript. The manuscript will undergo copyediting, typesetting, and review of the resulting proof before it is published in its final citable form. Please note that during the production process errors may be discovered which could affect the content, and all legal disclaimers that apply to the journal pertain.

Author Manuscript Author Manuscript Author Manuscript Author Manuscript

1. Introduction

Preservation of genomic integrity by the DNA repair response is fundamental to the function and survival of cells. The DNA damage response in post-mitotic neurons includes cell-cycle arrest coupled with DNA repair (Lavin et al., 2005, Friedberg, 2003). Accumulation of DNA breaks can result in apoptosis, senescence or aberrant differentiation. In this regard, several studies have suggested that defects in cell-cycle and DNA repair pathways lead to uncontrolled cell death and play an important role in the pathogenesis of several age-related neurodegenerative disorders (Adamec et al., 1999, Best, 2009, Chen et al., 2010, Gensler and Bernstein, 1981, Katsel et al., 2013, Ioannidou et al., 2016). Identification of genes and their encoded proteins critically involved in DNA checkpoints and repair within the central nervous system (CNS) establishes mechanistic precedents for unraveling the pathobiology of age-related deterioration in global neurological functioning (McKay et al., 2017, Seidler et al., 2010) and specific age-related neurological disorders including dementia (Silva et al., 2014, Saykin et al., 2015) and dystonia (Ledoux et al., 2013).

CDKN1A interacting zinc finger protein 1(CIZ1), a cell-cycle protein widely expressed in neural and extra-neural tissues, plays an important role in DNA synthesis at the G1/S cell-cycle checkpoint (Coverley et al., 2005, Liu et al., 2016, Mitsui et al., 1999) and localization of Xist RNA to the inactive X chromosome (Ridings-Figueroa et al., 2017). Depletion of CIZ1 transcripts restrains cell proliferation by inhibiting entry to S phase. *CIZ1* mutations are associated with isolated cervical dystonia, possibly by precipitating G1/S cell-cycle dysregulation in the mature human brain (Xiao et al., 2012). Young adult *Ciz1*$^{-/-}$ mice exhibit motoric and hematological abnormalities including elevated monocyte and neutrophil counts in peripheral blood (Xiao et al., 2016). Gene expression studies showed that transcription factor 7-like 2 (TCF7L2), a member of the Wnt/β-catenin signaling pathway, was a major hub for down-regulated genes, whereas NF-κB was a major hub for up-regulated genes in *Ciz1*$^{-/-}$ mouse brain, suggesting that CIZ1 deficiency is associated with synaptic plasticity and neurodegeneration. Besides its potential roles in dystonia and the maintenance and/or differentiation of post-mitotic neurons within the CNS, CIZ1 may also be an important contributor to several other neural and extra neural diseases (Higgins et al., 2012, Liu et al., 2015, Yin et al., 2013, Judex et al., 2003, Bageghni et al., 2017, Dahmcke et al., 2008, Warder and Keherly, 2003). For instance, dysfunction of CIZ1 caused by aberrant splicing of exon 8 may contribute to the pathogenesis of Alzheimer disease (AD) by inhibiting proliferation and differentiation of neural progenitor cells in the hippocampus (Dahmcke et al., 2008). In other studies, a *CIZ1* variant was found to be a circulating biomarker for early-stage lung cancer (Higgins et al., 2012) and overexpression of CIZ1 in the heart reduced the impact of myocardial injury (Bageghni et al., 2017). CIZ1 has been shown to co-regulate estrogen receptor α (ERα) by enhancing estrogen transactivation activity by promoting the recruitment of the estrogen complex to target gene chromatin (den Hollander et al., 2006). Estrogen binds to ERα and is neuroprotective in cellular and mouse models of neurodegeneration (Fitzpatrick et al., 2002, Rosario et al., 2010, Hwang et al., 2015).

The relationship of *CIZ1* variants to age-related neurological disorders (AD and adult-onset isolated dystonia) prompted us to use our *Ciz1* null mouse model to examine to role of

Author Manuscript Author Manuscript Author Manuscript Author Manuscript

defective cell-cycle control and associated DNA repair pathways in neurodegeneration. A growing literature has pointed to a potential role for defective DNA repair in human neurodegenerative disorders (Coppede and Migliore, 2009, Chow and Herrup, 2015, Ross and Truant, 2017) including dystonia (Ledoux et al., 2013, Prudente et al., 2013). Moreover, a significant percentage of human populations with dementia do not have AD-type pathology on postmortem brain examination (Grammas, 2011, Graff-Radford et al., 2016). Alternative mechanisms for dementia include the cumulative effects of neuronal loss due to defects in DNA repair pathways and microvascular dysfunction (Chui and Ramirez Gomez, 2017). Therefore, model systems to study DNA repair and neurovascular risk factors are essential for understanding global neurological decline.

Herein, we found that CIZ1 deficiency leads to cell-cycle dysfunction, the accumulation of DNA breaks, and increased apoptosis in mouse embryonic fibroblasts (MEFs). Aged *Ciz1*$^{-/-}$ mice showed persistent DNA breaks, motor and cognitive deficits, increased oxidative and inflammatory markers in brain, neurovascular dysfunction, and neuronal apoptosis. Overall, our data indicate that the deleterious effects of CIZ1 deficiency become more pronounced with aging and suggest that defects in cell-cycle checkpoints and associated DNA repair pathways may contribute to the pathobiology of neurodegenerative disorders and age-related global decline in neurological functioning.

2. Materials and methods

2.1. Cell Culture and irradiation

MEFs were isolated from embryos at 12 to 14 d gestation and grown and cultured in Dulbecco's modified Eagle's medium (DMEM) supplemented with 10% fetal bovine serum, 1% L-glutamine and 1% penicillin-streptomycin. Cells were plated on gelatin-coated T25 tissue culture flasks in an incubator at 37°C with 5% CO_2. After the fourth passage, MEFs were exposed to γ-radiation (0, 5, 10 and 20 Gy) using a ^{137}Cs source. In pilot experiments, we performed dose-response effects (5, 10 and 20 Gy) of γ-irradiation to establish the optimal dose of γ-irradiation (20 Gy) for comparative analysis of DNA damage. Immediately after irradiation, cells were returned to the incubator for recovery.

2.2. Analyses of DNA damage, the cell-cycle, and apoptosis

For assessment of DNA damage, cells were plated on poly-l-lysine-coated coverslips and fixed with 4% paraformaldehyde. After fixation, cells were washed twice with 1X phosphate-buffered saline (PBS) and permeabilized with 0.3% Triton X-100 for 15 min followed by blocking with 1% bovine serum albumin (BSA) in PBS. Cells were incubated with rabbit anti-phospho-H2A.X (Ser139) (#2577, Cell Signaling) or rabbit anti-53BP1 (ab21083, Abcam) for 2 h at room temperature, rinsed and incubated with a fluorescently-tagged secondary antibody (Jackson ImmunoResearch Laboratories) for 1 h and then washed 3X with PBS. Coverslips were mounted onto slides with medium containing DAPI (H-1200, Vector).

For cell-cycle analysis, cells were fixed with ice-chilled 70% ethanol for 1 h. Fixed cells were then washed with PBS 3X followed by incubation with PI staining buffer (50 μg/mL)

Author Manuscript Author Manuscript Author Manuscript Author Manuscript

for 30 min. After incubation, cells were analyzed by flow cytometry (BD Biosciences LSR II Flow Cytometer). FITC Annexin V/Dead Cell Apoptosis Kit (V13242, Thermofisher) was used to detect apoptosis in MEFs after irradiation according to the manufacturer's instructions. Briefly, cells were harvested, washed in cold PBS and then centrifuged to discard the supernatant. Pellets were suspended with 1X annexin-binding buffer. Cells were incubated with 5 μL of FITC annexin V and 1 μl of 100 μg/ml propidium iodide (PI) working solution for 15 min and then analyzed with a BD Biosciences LSR II Flow Cytometer.

2.3. Alkaline comet assay

To characterize DNA damage, the alkaline comet assay was performed on cultured MEFs after 4 passages using the protocol provided with Trevigen's Comet Assay kit. Comet assays were also performed on cells isolated from the brains of *Ciz1*$^{-/-}$ mice and their sex-matched littermates. The comet assay or single cell gel electrophoresis is a sensitive technique for quantifying DNA damage in individual cells. The resulting image resembles a comet with a head and tail. The tail contains broken DNA. Percent DNA in the tail or % tail DNA is a normalized measure of the percentage of total DNA found in the tail. Briefly, tissues were homogenized in a glass teflon dounce homogenizer by 10 strokes and cells were collected through a 100 μm cell strainer (ThermoFisher Scientific). In brief, 1×10^5 cells were mixed with 500 μl of pre-warmed low melting temperature agarose (1:10, v/v) and 50 μl of the mixture was plated onto slides (CometSlide™, Trevigen). After agarose solidified and attached to slides, slides were immersed in pre-chilled lysis solution for 1 h on ice, then in alkaline unwinding solution (200 mM NaOH, 1 mM EDTA) for 1 h at room temperature. Electrophoresis was performed in a pre-chilled alkaline electrophoresis solution (200 mM NaOH, 1 mM EDTA) at 4°C for 30 min at 21 V. Slides were then washed for 5 min with distilled water 2X, followed by a 5 min-incubation with 70% ethanol. Slides were air-dried at 37°C for 15 min in the dark and agarose gels were stained with SYBR® Gold for 5 min at 4°C. After SYBR Gold was removed and slides were air-dried, images were acquired with fluorescence microscopy. The DNA-bound SYBR® Gold emits green light when excited at 425 – 500 nm. Assays were carried out in triplicate and mean % tail DNA for at least 50 cells/slide was determined by two investigators blinded to genotype. Means were used for statistical comparisons.

2.4. Maintenance and breeding of mice

Ciz1$^{-/-}$ mice and *Ciz1*$^{+/+}$ littermates (18-mo-old) were used in the experiments described herein. *Ciz1*$^{-/-}$ founders were backcrossed to C57BL/6J mice for at least 6 generations and genotyped as previously described (Xiao et al., 2016). All experiments used *Ciz1*$^{+/+}$ littermates on the same genetic background. All mouse experiments were performed in accordance with the National Institutes of Health's Guidelines for the Care and Use of Laboratory Animals and approved by our Institutional Animal Care and Use Committee.

2.5. Behavioral assessments

Ciz1$^{-/-}$ mice and sex-matched *Ciz1*$^{+/+}$ littermates at 18-mo of age were subjected to a battery of sensorimotor and cognitive tests including open-field activity, rotarod, vertical rope climbing, raised-beam task, grip strength, dominance tube, cross maze and Morris

Author Manuscript Author Manuscript Author Manuscript Author Manuscript

water maze as previously described (Xiao et al., 2016, Xiao et al., 2017, Caccamo et al., 2014). Tests were performed by investigators blinded to genotype. An expanded version of these methods is available in the supporting information.

2.6. Immunohistochemistry

Ciz1$^{-/-}$ mice and WT littermates were overdosed with pentobarbital (> 100 mg/kg) and transcardially perfused, first with ice cold saline and then 4% paraformaldehyde in 0.1M phosphate buffer (PB, pH 7.4). Brains were removed, weighed and post-fixed with 4% paraformaldehyde and cryoprotected with 30% sucrose in 0.1M PBS. Brains were sectioned on a cryostat at 20 μm. Endogenous peroxidases were quenched with 1% H_2O_2 in PBS and sections were rinsed with PBS followed by blocking with 2% non-fat dry milk and 0.3% Triton X-100. Sections were incubated overnight with rat anti-mouse Ly-6B.2 monoclonal antibody (Bio-Rad, MCA771GT) followed by biotinylated goat anti-rat IgG (Vector Laboratories, BA-9400). After rinsing with PBS X 3, sections were developed using the Vectastain ABC Kit from Vector Laboratories and DAB (3,3'-diaminobenzidine). Sections were counterstained with hematoxylin. For immunofluorescence, we used primary antibodies to 53BP1 (ab21083, Abcam), ionized calcium binding adaptor molecule 1(Iba-1) [1:500, polyclonal rabbit, Wako- #019-19741], NeuN (1:100, mouse monoclonal, EMG Millipore - MAB377) and glial fibrillary acidic protein (GFAP) [1:500, polyclonal rabbit, Abcam - #7260]. One of the following fluorescent secondary antibodies was used: Alexa Flour 568 anti-rabbit, Alexa Flour 488 anti-rabbit. These sections were then washed and mounted with Vectashield® mounting medium containing DAPI (H-1200, Vector Labs). The numbers of GFAP and Iba-1 positive cells were counted at 400X magnification (4 or 5 fields/region and genotype) by an investigator blinded to genotype.

2.7. Western blot analyses

Dissected brain tissues and MEFs were lysed with ice-cold RIPA lysis buffer (ThermoFisher Scientific) containing Halt™ protease and phosphatase inhibitor cocktail (ThermoFisher Scientific). Lysed issue and cells samples were microcentrifuged for 15 min at 14,000 rpm and the supernatants were collected. Proteins were separated by SDS-PAGE (4–12% Bis-Tris gels) and transferred to PVDF membranes using a BioRad wet transfer system. Subsequently, membranes were blocked for 2 h in 5% non-fat dry milk and incubated overnight with rabbit anti-phospho-H2A.X (Ser139) (#2577, Cell Signaling) in tris-buffered saline with Tween 20 (TBST) or rabbit anti-4-hydroxynonenal (HNE) primary antibody (ab46545; Abcam) in phosphate-buffered saline with Tween 20 (PBST) containing 5% non-fat dry milk. Membranes were washed 3X with 1XTBST and 1X PBST respectively for 15 min and then incubated with horseradish peroxidase-conjugated goat anti-rabbit secondary antibody (Jackson ImmunoResearch Laboratories) for 1 h with constant rocking at room temperature. Signal was detected using enhanced chemiluminescence (Amersham) and quantified with NIH image J software.

2.8. Myeloperoxidase (MPO) activity assay

Brain tissues were sonicated in 50 mM potassium phosphate buffer containing 0.5% hexadecyltrimethylammonium bromide. After centrifugation, the supernatant was diluted in reaction solution containing o-dianisidine hydrochloride and H_2O_2. The rate of change in

Author Manuscript Author Manuscript Author Manuscript Author Manuscript

optical density (OD) for 1 min was measured at 460 nm to calculate MPO activity as previously described (Khan et al., 2017).

2.9. ELISAs

Mice were anesthetized with pentobarbital (> 100 mg/kg) and transcardially perfused with ice-cold saline and decapitated. Brains were collected and homogenized in tissue lysis buffer (50 mM Tris HCl, pH 8.0, 5 mM NaCl, and 1% Triton X-100) containing Halt™ protease and phosphatase inhibitor cocktail. Nuclear fractions were prepared with NE-PER™ nuclear and cytoplasmic extraction kit (ThermoFisher Scientific, #78833) according to the manufacturer's instructions. Briefly, lysed tissues were microcentrifuged for 5 min at 14,000 rpm and supernatants were collected for interleukin-6 (IL-6) and reduced glutathione (GSH) assays. Insoluble pellets were resuspended in ice-cold nuclear extraction reagent. Pellets were placed on ice and vortexed for 15 s every 10 min, for a total of 40 min. After incubation, pellets were microcentrifuged for 10 min at 14,000 rpm and nuclear fractions were collected for the analysis of NF-κB. Protein concentrations were determined using a bicinchoninic acid assay (BCA) kit (Thermo Fisher Scientific, #23227).

An IL-6 ELISA kit (R & D System, DY406-05) was used for determination of IL-6 levels in accordance with the manufacturer's instructions. Briefly, the capture antibody was diluted to the working concentration in PBS and used to load a 96-well microplate with 100 μL per well. The plate was sealed and incubated overnight at room temperature.. After washing, standards and samples were pipetted into the wells and incubated for 2 h. After washing away unbound substances, an enzyme linked polyclonal antibody specific for IL-6 was added to the wells. Following a wash to remove any unbound antibody–enzyme reagent, a substrate solution was added to the wells and color developed in proportion to the amount of bound IL-6. The reaction was terminated by the addition of 2N sulfuric acid. The absorbance was measured at 450 nm with a microtiter plate reader (SpectraMax M2e, Molecular Devices).

GSH was measured with a commercial ELISA kit (Cayman Chemical, #703002) in accordance with the manufacturer's instructions. Briefly, 50 μl of standards and samples were added to 150 μl of a reaction mixture containing nicotinamide adenine dinucleotide phosphate ($NADP^+$), glutathione reductase, glucose-6-phosphate, and 5,5′-dithiobis-2-nitrobenzoic acid (DTNB). The reaction was carried out at 37 °C for 10 min, and then GSH levels were determined by absorbance at 412 nm with a microtiter plate reader (SpectraMax M2e).

The activity of NF-κB was measured in nuclear extracts with a commercial NF-κB (p65) Transcription Factor Assay kit (Cayman Chemical, #10007889) in accordance with the manufacturer's instructions. Briefly, a specific double-stranded DNA sequence containing the NF-κB response element was immobilized to wells of a 96-well plate, nuclear fractions were added to wells, and NF-κB (p65) was detected by addition of a specific primary antibody. A secondary antibody conjugated to HRP was added to provide a sensitive colorimetric readout at 450 nm. Optical density was normalized using the amount of protein present in the nuclear fraction.

Author Manuscript Author Manuscript Author Manuscript Author Manuscript

2.10. Relative quantitative real-time reverse-transcriptase PCR (QRT-PCR) for expression of vascular adhesion factors

Relative levels of mouse intercellular adhesion molecule 1 (ICAM-1) and vascular adhesion molecule (VCAM) mRNA were determined in hippocampus harvested from 3 mice (18 mo) of each genotype (*Ciz1*$^{-/-}$ and *Ciz1*$^{+/+}$). TaqMan (Roche)-based QRT-PCR was performed using two primer pairs and probes (ICAM: forward, tggaagctgtttgagctgag; reverse, tgccacagttctcaaagcac; probe 56; VCAM, forward, gagaatgaacactcttacctgtgc; reverse, cacgtggatacttcgttccag; probe 21) with a LightCycler® 480 System (Roche). Mouse β-actin was used as the endogenous control.

2.11. Terminal deoxynucleotidyl transferase dUTP nick-end labeling (TUNEL)

TUNEL staining was performed using a commercially available *in situ* Cell Death Detection Kit (Roche Diagnostics). The assay was performed according to the manufacturer's instructions. Data were analyzed by determining the mean number of TUNEL-positive cells per 200X magnification field. A rater blinded to genotype examined eight microscopic fields per slide.

2.12. Statistical analysis

ANOVA with post-hoc tests was used to determine the effects of genotype and sex on parametric behavioral measures. ANOVA with post-hoc tests was used to determine the effects of genotype and radiation on % tail DNA. The Mann-Whitney test was used to determine the effects of genotype within sex for a non-parametric behavioral measure (slips on the raised beam task). Two-tailed *t*-tests were used to determine the effects of genotype on gene expression, TUNEL labeling, biochemical measures, and hematological parameters. Fisher's exact test was used to determine the effects of genotype on the results of dominance tube testing. An alpha (α) of 0.05 was chosen for statistical significance.

3. Results

3.1. CIZ1 deficiency causes persistent DNA damage, cell-cycle defects and apoptosis in MEFs

To determine the contributions of CIZ1 to the DNA damage response, we subjected MEFs isolated from *Ciz1*$^{+/+}$ (wild-type, WT) and *Ciz1*$^{-/-}$ (knock-out or null) mice to γ-irradiation. MEFs isolated from *Ciz1*$^{-/-}$ mice showed increased sensitivity to irradiation. At 24 hr after IR (20 Gy), we assessed the persistence of DNA break markers γ-H2A.X (ser139) and 53BP1 and degree of DNA damage with comet assays. MEFs isolated from null mice displayed increased and sustained γ-H2A.X(ser139)- (Fig. 1 *A* and *B*) and 53BP1- (Fig. S1) immunoreactivity. There were significant effects of irradiation ($F_{1,8}$ = 271,8, P < 0.0001) and genotype ($F_{1,8}$ = 13.8, P = 0.0059) on % tail DNA (Fig. 1 *C* and *D*). Using flow cytometry, MEFs from null mice showed cell-cycle defects (Fig. 1*E*) and increased apoptosis (two-tailed $t(8)$ = 3.14, P = 0.014; Fig. 1*F*) in comparsion with MEFs from WT littermates. In aggregate, these results indicate that CIZ1-deficient MEFs are more sensitive to irradiation than WT MEFs, as evidenced by increased DNA damage, cell-cycle disruption and cell death.

Author Manuscript Author Manuscript Author Manuscript Author Manuscript

3.2. CIZ1 deficiency is associated with DNA damage in the brains of aged mice

First, we confirmed that CIZ1 is widely expressed in neural tissue and present within nuclear foci in mouse neurons, astrocytes and microglia (Fig. S2). CIZ1 is known to interact with cyclin A1 (Greaves et al., 2012), a cell-cycle protein implicated in the repair of DNA double-strand breaks (DSBs). Therefore, we sought to determine if CIZ1 deficiency contributes to impaired DNA repair in brain. For this purpose, we investigated DNA damage in the cerebellum and hippocampus of aged WT and null mice with comet assays (Fig. 2*A–D*) and immunohistochemistry (Fig. 2*F–I*). We found increased % tail DNA (Fig. 2*E*) in the cerebellum (two-tailed $t(10) = 12.14$, $P < 0.0001$) and hippocampus (two-tailed $t(10) = 14.07$, $P < 0.0001$) of aged *Ciz1*$^{-/-}$ mice as compared with WT littermates. Similarly, 53BP1-immunoreactive cells (Fig. 2*J*) were also more prevalent in the cerebellum (two-tailed $t(4) = 4.90$, $P = 0.008$) and hippocampus (two-tailed $t(5) = 4.12$, $P = 0.0091$) of aged *Ciz1*$^{-/-}$ mice. Taken together, these results implicate CIZ1 as a participant in the DNA damage response.

3.3. Oxidative stress is seen in the brains of aged Ciz1$^{-/-}$ mice

Oxidative stress generally refers to increased levels of reactive oxygen species (ROS) which can damage DNA, RNA, proteins and lipids. Oxidative stress, most commonly linked to impaired mitochondrial function, plays an important role in the pathogenesis of aging and neurodegeneration (Gibson et al., 2008, Butterfield et al., 2001). ROS are a major cause of DSBs and other deleterious changes to DNA. Analysis of lipid peroxidation (LPO) and GSH levels in *Ciz1*$^{-/-}$ mice was motivated by the known functional interplay between the cell-cycle, DNA damage response and oxidative stress (Yan et al., 2014). LPO, a classic marker of oxidative stress, is seen in the earliest stages of neurodegeneration (Bradley-Whitman and Lovell, 2015). Levels of the antioxidant glutathione, which is essential for detoxification of ROS, are commonly reduced in neurodegenerative diseases (Mazzetti et al., 2015). In comparison to WT littermates, *Ciz1*$^{-/-}$ mice exhibited increased LPO (two-tailed $t(4) = 4.14$, $P = 0.014$) and decreased GSH (two-tailed $t(7) = 2.56$, $P = 0.037$) levels (Fig. 3 *A* and *B*).

3.4. Aged Ciz1$^{-/-}$ mice show increased glial activation in the CNS

Activation of microglia and astrocytes, hallmarks of neuroinflammation, has been reported in several neurodegenerative disorders (Glass et al., 2010, Khan et al., 2015). In the present study, we analyzed astrocytic (GFAP) and microglial (Iba1) activation in the brains (cerebellum and hippocampus) of aged *Ciz1*$^{-/-}$ mice and WT littermates. GFAP immunostaining exposed astroglial activation and increased numbers of activated astrocytes in the cerebellae (two-tailed $t(4) = 3.67$, $P = 0.021$) of *Ciz1*$^{-/-}$ mice as compared with WT littermates (Fig. 4). Differences did not reach statistical significance in the hippocampi (two-tailed $t(4) = 2.17$, $P = 0.096$). There were significantly increased numbers and amoeboid features of Iba1-positive activated microglia in *Ciz1*$^{-/-}$ mice compared with WT littermates in both the cerebellum (two-tailed $t(3) = 8.92$, $P = 0.0030$) and hippocampus (two-tailed $t(4) = 3.93$, $P = 0.017$) (Fig. 4).

Author Manuscript Author Manuscript Author Manuscript Author Manuscript

3.5. NF-κB is up-regulated in Ciz1$^{-/-}$ mice

NF-κB signaling is at the center of the inflammatory network in aging and plays an important role in myriad physiological and pathophysiological conditions (Mattson and Camandola, 2001, Bauernfeind et al., 2009). In previous work using gene-expression microarrays, we found that NF-κB was a major hub for up-regulated genes in *Ciz1*$^{-/-}$ mice (Xiao et al., 2016). Consistent with our gene expression data, we observed increased protein levels of NF-κB (p65) in the nuclear extracts from the cerebellae (two-tailed $t(9) = 5.18$, $P = 0.0006$) and hippocampi (two-tailed $t(7) = 5.02$, $P < 0.0015$) of aged *Ciz1*$^{-/-}$ mice as compared with WT littermates (Fig. S3).

3.6. CIZ1 deficiency triggers inflammation

We then tested the hypothesis that increased DNA damage and NF-κB upregulation are associated with increased neuroinflammation. For this purpose, we analyzed MPO activity and proinflammatory cytokine IL-6 levels in supernatant fractions of brain (Fig. S4). MPO, an abundant pro-inflammatory enzyme stored in neutrophils and monocytes, is also expressed by perivascular macrophages and amoeboid microglia in the CNS (Kaindlstorfer et al., 2015). MPO-immunoreactive cells are prominent in brain regions undergoing neurodegeneration in Parkinson and Alzheimer diseases (Gellhaar et al., 2017). The pro-inflammatory cytokine IL-6 is elevated in both classic neurodegenerative disorders like Parkinson and AD and primary neuroinflammatory conditions such as multiple sclerosis (Alam et al., 2016). IL-6 signaling promotes DNA repair (Chen et al., 2015). Neutrophils were more abundant in the brains of *Ciz1*$^{-/-}$ mice compared with WT littermates (Fig. S4 *A*), and *Ciz1*$^{-/-}$ mice demonstrated significantly increased MPO activity (two-tailed $t(10) = 2.83$, $P = 0.018$; Fig. S4 B) and IL-6 levels (two-tailed $t(13) = 2.26$, $P = 0.042$; Fig. S4 *C*). We also observed a significantly increased percentage of neutrophils in the blood of aged *Ciz1*$^{-/-}$ female mice compared with WT female littermates (two-tailed $t(10) = 5.25$, $P = 0.0004$; Table S1). These findings demonstrate that CIZ1 deficiency triggers inflammatory responses.

3.7. Aged Ciz1 null mice show evidence of neurovascular dysfunction

To determine if CIZ1 deficiency causes endothelial dysfunction, we measured the expression of ICAM-1 and VCAM with QRT-PCR. Induction of ICAM-1 and VCAM expression are well-established markers of endothelial cell activation and vascular dysfunction (Engelhardt et al., 1994, Seo et al., 2015). VCAM levels are elevated in patients with both Alzheimer and vascular dementia (Zuliani et al., 2008). Aged *Ciz1* null mice showed higher expression levels of ICAM (two-tailed $t(7) = 4.47$, $P = 0.0029$) and VCAM (two-tailed $t(7) = 2.72$, $P = 0.030$) compared with WT littermates (Fig. S5).

3.8. Deficiency of CIZ1 is associated with cell death in the brains of aged mice

Next, we tested the hypothesis that the accumulation of DNA breaks contributes to cell death in *Ciz1*$^{-/-}$ mice. TUNEL labeling showed that markers of DNA damage, inflammation, and neurovascular dysfunction were accompanied by increased apoptosis in sensorimotor (cerebellum; two-tailed $t(9) = 5.18$, $P = 0.0006$) and cognitive (hippocampus; two-tailed $t(7)$

Author Manuscript Author Manuscript Author Manuscript Author Manuscript

= 5.02, $P = 0.0015$) regions of the CNS in *Ciz1* null mice in comparison with WT littermates (Fig. 5).

3.9. CIZ1 deficiency contributes to sensorimotor, behavioral, and cognitive deficits in aged mice

Our earlier work showed that CIZ1 deficiency causes mild motor abnormalities in 3-mo-old mice (Xiao et al., 2016). Now, we provide multiple lines of evidence that aged (18-mo-old) *Ciz1* mice exhibit marked relative deficits in sensorimotor and behavioral functioning in comparison with WT littermates. There were no overall effects of genotype on body or brain weights (Table S2, Fig. S6). In comparison with WT littermates, both male ($F_{1,31} = 11.19$, $P = 0.0022$) and female ($F_{1,31} = 12.63$, $P = 0.0024$) $Ciz1^{-/-}$ mice performed poorly on the rotarod (Fig. 6*A*) and raised-beam tasks (Fig. 6 *B* and *C*). On the 12-mm square beam, there were overall effects of genotype ($F_{1,41} = 20.10$, $P < 0.0001$) and sex ($F_{1,41} = 10.54$, $P < 0.0023$) on traversal times but no genotype*sex interaction. On the 12-mm round beam, there were overall effects of genotype ($F_{1,40} = 37.14$, $P < 0.0001$) and sex ($F_{1,40} = 19.29$, $P < 0.0001$) on traversal times and a weak genotype*sex interaction ($F_{1,40} = 4.12$, $P < 0.049$) with relatively poorer performances by female than male $Ciz1^{-/-}$ mice. Analysis of slips with the Mann-Whitney U statistic exposed similar effects of genotype on performance. On the 12-mm square beam, both male (Mann-Whitney U = 16, $P = 0.0002$) and female (Mann-Whitney U = 1, $P < 0.0001$) $Ciz1^{-/-}$ mice exhibited more slips than their WT littermates (Fig. 6*C*). Likewise, on the 12-mm round beam, both male (Mann-Whitney U = 10, $P < 0.0001$) and female (Mann-Whitney U = 14, $P < 0.018$) $Ciz1^{-/-}$ mice exhibited more slips than WT littermates (Fig. 6*C*). There was no overall effect of genotype on grip strength or normalized grip strength. However, normalized grip strength showed a significant genotype*gender interaction ($F_{1,48} = 8.38$, $P = 0.0057$) with female $Ciz1^{-/-}$ mice showing lower values for grip strength/body weight in comparision with WT littermates ($P = 0.011$). A similar genotype*gender interaction ($F_{1,30} = 11.88$, $P = 0.0017$) was seen for normalized rope climbing times with female $Ciz1^{-/-}$ mice showing larger values for rope climbing time/body weight in comparision with WT littermates ($P = 0.003$).

Overall, male mice were more active than female mice, particularly in the vertical plane, and $Ciz1^{-/-}$ mice were less active than their WT littermates (Table S2). $Ciz1^{-/-}$ mice traveled shorter distances ($F_{1,48} = 16.99$, $P < 0.0001$), had lower ambulatory counts ($F_{1,48} = 16.45$, $P = 0.0002$) and fewer ambulatory episodes ($F_{1,48} = 11.69$, $P = 0.0013$) than their WT littermates in the open field and there were no differential effects of sex for any of these three measures. Likewise, there were overall effects of genotype on stereotypic ($F_{1,48} = 17.68$, $P < 0.0001$), vertical ($F_{1,48} = 5.58$, $P = 0.022$) and jump ($F_{1,48} = 10.49$, $P = 0.0022$) counts. The genotype*sex interaction ($F_{1,48} = 6.63$, $P = 0.013$) reached statistical significance for jump counts with more pronounced relative reductions in male than female $Ciz1^{-/-}$ mice. There was no overall effect of genotype on average velocity but post-hoc analyses showed the male $Ciz1^{-/-}$ mice were slower than their WT male littermates ($P = 0.028$).

Behaviorally, male and female $Ciz1^{-/-}$ mice were more aggressive than their WT littermates in the dominance tube ($P < 0.0001$, for both; Table S2). Similar to motor and behavioral

Author Manuscript Author Manuscript Author Manuscript Author Manuscript

findings, we also observed cognitive dysfunction in *Ciz1*$^{-/-}$ mice as assessed by cross maze and Morris water maze testing (Fig. 6*D–F*). The was an overall effect of genotype ($F_{1,31}$ = 24.61, $P < 0.0001$) but no effect of sex or the genotype*sex interaction on cross maze scores. There were modest effects of the null genotype on escape latencies in both male ($F_{1,14}$ = 4.38, $P = 0.054$) and female ($F_{1,14}$ = 4.65, $P = 0.049$) mice. There was a strong overall effect of the null genotype on the probe trial (Fig. 6*F*; $F_{1,26}$ = 14.17, $P = 0.0009$) but no effect of the genotype*sex interaction. These data indicate that the deleterious effects of CIZ1 deficiency become more pronounced with aging and CIZ1 deficiency contributes to the development of both cognitive and motor dysfunction.

4. Discussion

Several studies have demonstrated the roles of ectopic cell-cycle events and DNA damage in neuropathological conditions and altered expression of cell-cycle proteins has been signified as a contributor to and indicator of cell death (Suberbielle et al., 2015, Katsel et al., 2013, Shen et al., 2016). CDKN1A-interacting zinc finger protein-1 (CIZ1), a nuclear protein that plays an important role in DNA replication and cell-cycle progression (Mitsui et al., 1999, Coverley et al., 2005), has been linked to cervical dystonia through G1/S cell-cycle dysregulation in humans (Xiao et al., 2012). Recently, we reported that germline knock-out of *Ciz1* causes motor and hematological abnormalities in young adult mice (Xiao et al., 2016). However, our previous work did not explore the significance of CIZ1 deficiency in the aged nervous system or contributions of CIZ1 to DNA repair pathways. In the present study, we learned that CIZ1 deficiency leads to impaired DNA repair capacity, cell-cycle defects, and apoptosis in MEFs. Concordant results were identified in the brains of aged *Ciz1* null mice with increased DNA breaks accompanied by neuroinflammation, vascular dysfunction, and cell death. Consistent with the effects of CIZ1 deficiency at the cellular level, aged *Ciz1* null mice had overt deficits in motor and cognitive functioning. Our findings expand upon previous work linking cell-cycle proteins to the DNA damage response in post-mitotic neurons (Suberbielle et al., 2015, Jordan-Sciutto et al., 2003, Kim and Tsai, 2009, Katsel et al., 2013, Shen et al., 2016) by tying a monogenic defect to the complete constellation of motor, cognitive, neurovascular, and neuroinflammatory phenotypes seen in age-related global neurological deterioration and neurodegenerative disorders. It should be noted, however, that young controls were not included in our experimental design and the influence of age and the age*genotype interaction on phenotypes was not directly tested by assessing *Ciz1*$^{+/+}$ and *Ciz1*$^{-/-}$ mice at multiple development time points.

DNA is constantly subjected to damage from numerous sources and defects in DNA repair processes can lead to senescence and uncontrolled cell death. However, neurons and other cell types within the CNS are equipped with a complex network of DNA repair mechanisms to preserve genomic integrity (Friedberg, 2003, Chow and Herrup, 2015). To understand the role of the cell-cycle protein CIZ1 in DNA damage response pathways, we first isolated MEFs from WT and *Ciz1*$^{-/-}$ mice. We found that MEFs isolated from *Ciz1*$^{-/-}$ mice were abnormally sensitive to γ-irradiation. Following irradiation, MEFs from *Ciz1*$^{-/-}$ mice displayed increased DNA damage, cell cycle defects, and increased apoptosis. In particular,

Author Manuscript Author Manuscript Author Manuscript Author Manuscript

we found persistent 53BP1 and γ-H2A.X-immunoreactivity at the sites of DSBs along with increased % tail DNA with comet assays (Rogakou et al., 1998, Lips and Kaina, 2001).

Mutations in genes that encode proteins involved in the cell-cycle and DNA repair have been linked to several age-related neurodegenerative and/or neurodevelopmental disorders including AD, ataxia telangiectasia (*ATM*), Cockayne syndrome (*ERCC8*), and xeroderma pigmentosum (*ERCC4*) (Best, 2009, Jeppesen et al., 2011, Katsel et al., 2013). Moreover, genome-wide association studies have consistently identified variants in cell-cycle genes as susceptibility factors for mild cognitive impairment and dementia (Saykin et al., 2015) and two polymorphisms in *CDKN1A* are associated with increased risk and earlier age-of-onset of AD (Yates et al., 2015). *ATM* shows interesting parallels to *CIZ1*. Both genes encode G1/S cell-cycle proteins and sequence variants in both genes have been linked to isolated dystonia and neoplasias. Loss of ATM in rats leads to accumulation of unrepaired DNA, increased cytokine production and activation of microglia (Quek et al., 2017a). Innate recognition of cytosolic self-DNA may trigger neuroinflammation in ATM and CIZ1 deficient rodents (Quek et al., 2017b, Li et al., 2017).

Among the types of DNA damage induced by ionizing radiation, DSBs may be the most lethal. DSBs are particularly deleterious in neurons because of their reduced DNA repair capacity when compared with proliferating cells (Kanungo, 2013). The accumulation of DNA damage is believed to result in a slow build-up of DNA adducts which may trigger an immune system response and inflammation and contribute to cell death (Ioannidou et al., 2016, Gasser and Raulet, 2006, Paludan, 2015). Deficiency of the cell-cycle protein ATM is associated with genomic instability and contributes neuronal death in mouse and human AD brain (Shen et al., 2016). Similarly, reduced neuronal expression of BRCA1 occurs in AD brain, causes cognitive dysfunction in mice and is characterized by sustained DSBs and abnormal chromatin remodeling (Suberbielle et al., 2015). Consistent with studies of the G1/S cell-cycle proteins ATM and BRCA1, our aged *Ciz1*$^{-/-}$ mice displayed increased DNA damage in the brain as demonstrated with persistent 53BP1-positive cells and increased percentages of DNA tails in neurons. The presence of extensive DNA damage and neuroinflammation in the aged brain may be manifestations of defective DNA repair pathways and accumulative oxidative damage to DNA (Silva et al., 2014, Chen et al., 2010).

Brain lipids, proteins and DNA are sensitive to oxidative stress (Radak et al., 2011, Butterfield et al., 2001, Markesbery and Lovell, 2007). In our study, we found a significant association between CIZ1 deficiency and oxidative stress in the brains of aged mice. *Ciz1*$^{-/-}$ mice exhibited increased LPO and decreased GSH. Oxidative damage to lipids can lead to structural and functional disruption of cell membranes and inactivation of enzymes, which ultimately leads to cell death. A reduction in GSH may impair H_2O_2 clearance and increases the free radical load, which promotes oxidative stress and consequently disrupts homeostasis. Moreover, altered cellular redox status can activate redox-sensitive transcription factors such as NF-κB (Janssen-Heininger et al., 2000). In view of our aggregate findings, it is worth considering the possibility that the increased oxidative stress identified in *Ciz1*$^{-/-}$ mice works as an amplification loop to further accelerate DNA damage and neurodegeneration.

Author Manuscript Author Manuscript Author Manuscript Author Manuscript

The importance of glia and pro-inflammatory mediators in neurodegenerative diseases has been supported by the analysis of diseased postmortem brains (Ouchi et al., 2009, Glass et al., 2010). Importantly, causal relationships between the accumulation of damaged DNA, glial activation, and age-related neurodegeneration was provided by work with *Ercc1* mutant mice (*Ercc1Δ/−*) (Borgesius et al., 2011). Consistent with study of ERCC1 which is involved in multiple DNA repair pathways, we observed that aged *Ciz1*$^{-/-}$ mice harbored more activated astrocytes and microglia than their WT littermates.

NF-κB, a master regulator of inflammation, plays an important role in myriad physiological and pathological conditions (Mattson and Camandola, 2001, Balistreri et al., 2013). NF-κB is upregulated in response to accumulation of damaged DNA and pharmacological inhibition of NF-κB activation leads to attenuation of age-related pathologies (Tilstra et al., 2012). Moreover, several studies have suggested that activated microglia also upregulate NF-κB nuclear translocation and inhibition of NF-κB suppresses pro-inflammatory cytokines and neuronal loss in mouse models of neurodegenerative diseases (Frakes et al., 2014, Khan et al., 2015, Ghosh et al., 2007). Consistent with our gene expression data in younger *Ciz1*$^{-/-}$ mice, we observed increased NF-κB (p65) and cytokine IL-6 in the brains of aged *Ciz1*$^{-/-}$ mice as compared with WT littermates. Furthermore, we provided evidence that upregulation of NF-κB was associated with damaged DNA and neuronal death in *Ciz1*$^{-/-}$ mice. Neutrophil influx into the CNS has been positively correlated with neuroinflammation and neuronal death (Khan et al., 2012, Soehnlein et al., 2017, Zenaro et al., 2015). In our study, we found that aged *Ciz1*$^{-/-}$ mice display increased MPO activity and neutrophil recruitment into the CNS as compared with their WT littermates. Although not assessed in our study, aged female *Ciz1*$^{-/-}$ mice have been reported to exhibit pathological evidence of a diffuse lymphoproliferative disorder resembling non-Hodgkin follicular-type lymphoma with enlarged organs, particularly the spleen (Ridings-Figueroa et al., 2017).

Recent studies have provided evidence that the accumulation of DNA breaks may be a direct contributor to neurovascular damage in several pathological conditions (Uryga et al., 2016, Bautista-Nino et al., 2016). In aged *Ciz1*$^{-/-}$ mice, we observed increased expression of ICAM1 and VCAM when compared with WT littermates. Increased expression of VACM-1 and ICAM-1 has been associated with increased risk of metabolic disorders and cognitive impairment (Hall et al., 2013, Zuliani et al., 2008).

Behavioral findings are often closely correlated with overall measures of CNS pathology in both humans and mice. Aged *Ciz1*$^{-/-}$ mice exhibited motor deficits on the rotarod, grip strength, rope climbing, open field activity, and a raised-beam task. *Ciz1*$^{-/-}$ mice also displayed cognitive deficits as measured by cross and Morris water mazes when compared with WT littermates. Our findings correlate well with our analyses of young adult *Ciz1*$^{-/-}$ mice and work with other mouse models in which motor and cognitive deficits were tied to defective cell-cycle proteins and DNA damage repair pathways (Xiao et al., 2016, Suberbielle et al., 2015).

Our findings that lack of CIZ1 is associated with the accumulation of damaged DNA and neurodegeneration in aged mice was not unexpected given CIZ1's established roles in DNA replication and cell-cycle progression at the G1/S checkpoint in mitotic cells. However, its

Author Manuscript Author Manuscript Author Manuscript Author Manuscript

role in aged post-mitotic neurons had not been investigated. Our study exposes an important role for the cell-cycle protein CIZ1 in the DNA damage repair pathways of post-mitotic neurons and potential contributions of CIZ1 and associated cell-cycle proteins to dementia. Overall, our results provide, for the first time, a rationale model system for studying the aggregate and combinatorial effects of DNA damage and neuroinflammation in global neurological decline in elderly human populations. Additional work will be required to determine the exact mechanisms through which CIZ1 contributes to DNA repair in the adult brain and delineate pathways linking DNA damage, neuroinflammation and vascular dysfunction.

Supplementary Material

Refer to Web version on PubMed Central for supplementary material.

Acknowledgments

This study was supported by the Neuroscience Institute at the University of Tennessee Health Science Center, Dystonia Medical Research Foundation, Dorothy/Daniel Gerwin Parkinson Research Fund, Department of Defense grant W81XWH-17-1-0062 and National Institutes of Health grants R01 NS082296 and R21 GM118962.

References

ADAMEC E, VONSATTEL JP, NIXON RA. DNA strand breaks in Alzheimer's disease. Brain Res. 1999; 849:67–77. [PubMed: 10592288]

ALAM Q, ALAM MZ, MUSHTAQ G, DAMANHOURI GA, RASOOL M, KAMAL MA, HAQUE A. Inflammatory Process in Alzheimer's and Parkinson's Diseases: Central Role of Cytokines. Curr Pharm Des. 2016; 22:541–8. [PubMed: 26601965]

BAGEGHNI SA, FRENTZOU GA, DRINKHILL MJ, MANSFIELD W, COVERLEY D, AINSCOUGH JF. Cardiomyocyte--specific expression of the nuclear matrix protein, CIZ1, stimulates production of mono-nucleated cells with an extended window of proliferation in the postnatal mouse heart. Biol Open. 2017; 6:92–99. [PubMed: 27934662]

BALISTRERI CR, CANDORE G, ACCARDI G, COLONNA-ROMANO G, LIO D. NF-kappaB pathway activators as potential ageing biomarkers: targets for new therapeutic strategies. Immun Ageing. 2013; 10:24. [PubMed: 23786653]

BAUERNFEIND FG, HORVATH G, STUTZ A, ALNEMRI ES, MACDONALD K, SPEERT D, FERNANDES-ALNEMRI T, WU J, MONKS BG, FITZGERALD KA, HORNUNG V, LATZ E. Cutting edge: NF-kappaB activating pattern recognition and cytokine receptors license NLRP3 inflammasome activation by regulating NLRP3 expression. J Immunol. 2009; 183:787–91. [PubMed: 19570822]

BAUTISTA-NINO PK, PORTILLA-FERNANDEZ E, VAUGHAN DE, DANSER AH, ROKS AJ. DNA Damage: A Main Determinant of Vascular Aging. Int J Mol Sci. 2016:17.

BEST BP. Nuclear DNA damage as a direct cause of aging. Rejuvenation Res. 2009; 12:199–208. [PubMed: 19594328]

BORGESIUS NZ, DE WAARD MC, VAN DER PLUIJM I, OMRANI A, ZONDAG GC, VAN DER HORST GT, MELTON DW, HOEIJMAKERS JH, JAARSMA D, ELGERSMA Y. Accelerated age-related cognitive decline and neurodegeneration, caused by deficient DNA repair. J Neurosci. 2011; 31:12543–53. [PubMed: 21880916]

BRADLEY-WHITMAN MA, LOVELL MA. Biomarkers of lipid peroxidation in Alzheimer disease (AD): an update. Arch Toxicol. 2015; 89:1035–44. [PubMed: 25895140]

BUTTERFIELD DA, DRAKE J, POCERNICH C, CASTEGNA A. Evidence of oxidative damage in Alzheimer's disease brain: central role for amyloid beta-peptide. Trends Mol Med. 2001; 7:548–54. [PubMed: 11733217]

Author Manuscript Author Manuscript Author Manuscript Author Manuscript

CACCAMO A, DE PINTO V, MESSINA A, BRANCA C, ODDO S. Genetic reduction of mammalian target of rapamycin ameliorates Alzheimer's disease-like cognitive and pathological deficits by restoring hippocampal gene expression signature. J Neurosci. 2014; 34:7988–98. [PubMed: 24899720]

CHEN J, COHEN ML, LERNER AJ, YANG Y, HERRUP K. DNA damage and cell cycle events implicate cerebellar dentate nucleus neurons as targets of Alzheimer's disease. Mol Neurodegener. 2010; 5:60. [PubMed: 21172027]

CHEN Y, ZHANG F, TSAI Y, YANG X, YANG L, DUAN S, WANG X, KENG P, LEE SO. IL-6 signaling promotes DNA repair and prevents apoptosis in CD133+ stem-like cells of lung cancer after radiation. Radiat Oncol. 2015; 10:227. [PubMed: 26572130]

CHOW HM, HERRUP K. Genomic integrity and the ageing brain. Nat Rev Neurosci. 2015; 16:672–84. [PubMed: 26462757]

CHUI HC, RAMIREZ GOMEZ L. Vascular Contributions to Cognitive Impairment in Late Life. Neurol Clin. 2017; 35:295–323. [PubMed: 28410661]

COPPEDE F, MIGLIORE L. DNA damage and repair in Alzheimer's disease. Curr Alzheimer Res. 2009; 6:36–47. [PubMed: 19199873]

COVERLEY D, MARR J, AINSCOUGH J. Ciz1 promotes mammalian DNA replication. J Cell Sci. 2005; 118:101–12. [PubMed: 15585571]

DAHMCKE CM, BUCHMANN-MOLLER S, JENSEN NA, MITCHELMORE C. Altered splicing in exon 8 of the DNA replication factor CIZ1 affects subnuclear distribution and is associated with Alzheimer's disease. Mol Cell Neurosci. 2008; 38:589–94. [PubMed: 18583151]

DEN HOLLANDER P, RAYALA SK, COVERLEY D, KUMAR R. Ciz1, a Novel DNA-binding coactivator of the estrogen receptor alpha, confers hypersensitivity to estrogen action. Cancer Res. 2006; 66:11021–9. [PubMed: 17108141]

ENGELHARDT B, CONLEY FK, BUTCHER EC. Cell adhesion molecules on vessels during inflammation in the mouse central nervous system. J Neuroimmunol. 1994; 51:199–208. [PubMed: 7514186]

FITZPATRICK JL, MIZE AL, WADE CB, HARRIS JA, SHAPIRO RA, DORSA DM. Estrogen-mediated neuroprotection against beta-amyloid toxicity requires expression of estrogen receptor alpha or beta and activation of the MAPK pathway. J Neurochem. 2002; 82:674–82. [PubMed: 12153491]

FRAKES AE, FERRAIUOLO L, HAIDET-PHILLIPS AM, SCHMELZER L, BRAUN L, MIRANDA CJ, LADNER KJ, BEVAN AK, FOUST KD, GODBOUT JP, POPOVICH PG, GUTTRIDGE DC, KASPAR BK. Microglia induce motor neuron death via the classical NF-kappaB pathway in amyotrophic lateral sclerosis. Neuron. 2014; 81:1009–23. [PubMed: 24607225]

FRIEDBERG EC. DNA damage and repair. Nature. 2003; 421:436–40. [PubMed: 12540918]

GASSER S, RAULET DH. The DNA damage response arouses the immune system. Cancer Res. 2006; 66:3959–62. [PubMed: 16618710]

GELLHAAR S, SUNNEMARK D, ERIKSSON H, OLSON L, GALTER D. Myeloperoxidase-immunoreactive cells are significantly increased in brain areas affected by neurodegeneration in Parkinson's and Alzheimer's disease. Cell Tissue Res. 2017

GENSLER HL, BERNSTEIN H. DNA damage as the primary cause of aging. Q Rev Biol. 1981; 56:279–303. [PubMed: 7031747]

GHOSH A, ROY A, LIU X, KORDOWER JH, MUFSON EJ, HARTLEY DM, GHOSH S, MOSLEY RL, GENDELMAN HE, PAHAN K. Selective inhibition of NF-kappaB activation prevents dopaminergic neuronal loss in a mouse model of Parkinson's disease. Proc Natl Acad Sci U S A. 2007; 104:18754–9. [PubMed: 18000063]

GIBSON GE, RATAN RR, BEAL MF. Mitochondria and oxidative stress in neurodegenerative disorders. Preface. Ann N Y Acad Sci. 2008; 1147:xi–xii. [PubMed: 19076425]

GLASS CK, SAIJO K, WINNER B, MARCHETTO MC, GAGE FH. Mechanisms underlying inflammation in neurodegeneration. Cell. 2010; 140:918–34. [PubMed: 20303880]

GRAFF-RADFORD NR, BESSER LM, CROOK JE, KUKULL WA, DICKSON DW. Neuropathologic differences by race from the National Alzheimer's Coordinating Center. Alzheimers Dement. 2016; 12:669–77. [PubMed: 27094726]

Author Manuscript Author Manuscript Author Manuscript Author Manuscript

GRAMMAS P. Neurovascular dysfunction, inflammation and endothelial activation: implications for the pathogenesis of Alzheimer's disease. J Neuroinflammation. 2011; 8:26. [PubMed: 21439035]

GREAVES EA, COPELAND NA, COVERLEY D, AINSCOUGH JF. Cancer-associated variant expression and interaction of CIZ1 with cyclin A1 in differentiating male germ cells. J Cell Sci. 2012; 125:2466–77. [PubMed: 22366453]

HALL JR, WIECHMANN AR, JOHNSON LA, EDWARDS M, BARBER RC, WINTER AS, SINGH M, O'BRYANT SE. Biomarkers of vascular risk, systemic inflammation, and microvascular pathology and neuropsychiatric symptoms in Alzheimer's disease. J Alzheimers Dis. 2013; 35:363–71. [PubMed: 23403534]

HIGGINS G, ROPER KM, WATSON IJ, BLACKHALL FH, ROM WN, PASS HI, AINSCOUGH JF, COVERLEY D. Variant Ciz1 is a circulating biomarker for early-stage lung cancer. Proc Natl Acad Sci U S A. 2012; 109:E3128–35. [PubMed: 23074256]

HWANG CJ, YUN HM, PARK KR, SONG JK, SEO HO, HYUN BK, CHOI DY, YOO HS, OH KW, HWANG DY, HAN SB, HONG JT. Memory Impairment in Estrogen Receptor alpha Knockout Mice Through Accumulation of Amyloid-beta Peptides. Mol Neurobiol. 2015; 52:176–86. [PubMed: 25128029]

IOANNIDOU A, GOULIELMAKI E, GARINIS GA. DNA Damage: From Chronic Inflammation to Age-Related Deterioration. Front Genet. 2016; 7:187. [PubMed: 27826317]

JANSSEN-HEININGER YM, POYNTER ME, BAEUERLE PA. Recent advances towards understanding redox mechanisms in the activation of nuclear factor kappaB. Free Radic Biol Med. 2000; 28:1317–27. [PubMed: 10924851]

JEPPESEN DK, BOHR VA, STEVNSNER T. DNA repair deficiency in neurodegeneration. Prog Neurobiol. 2011; 94:166–200. [PubMed: 21550379]

JORDAN-SCIUTTO KL, DORSEY R, CHALOVICH EM, HAMMOND RR, ACHIM CL. Expression patterns of retinoblastoma protein in Parkinson disease. J Neuropathol Exp Neurol. 2003; 62:68–74. [PubMed: 12528819]

JUDEX M, NEUMANN E, LECHNER S, DIETMAIER W, BALLHORN W, GRIFKA J, GAY S, SCHOLMERICH J, KULLMANN F, MULLER-LADNER U. Laser-mediated microdissection facilitates analysis of area-specific gene expression in rheumatoid synovium. Arthritis Rheum. 2003; 48:97–102. [PubMed: 12528109]

KAINDLSTORFER C, SOMMER P, GEORGIEVSKA B, MATHER RJ, KUGLER AR, POEWE W, WENNING GK, STEFANOVA N. Failure of Neuroprotection Despite Microglial Suppression by Delayed-Start Myeloperoxidase Inhibition in a Model of Advanced Multiple System Atrophy: Clinical Implications. Neurotox Res. 2015; 28:185–94. [PubMed: 26194617]

KANUNGO J. DNA-dependent protein kinase and DNA repair: relevance to Alzheimer's disease. Alzheimers Res Ther. 2013; 5:13. [PubMed: 23566654]

KATSEL P, TAN W, FAM P, PUROHIT DP, HAROUTUNIAN V. Cell cycle checkpoint abnormalities during dementia: A plausible association with the loss of protection against oxidative stress in Alzheimer's disease [corrected]. PLoS One. 2013; 8:e68361. [PubMed: 23861893]

KHAN MM, GANDHI C, CHAUHAN N, STEVENS JW, MOTTO DG, LENTZ SR, CHAUHAN AK. Alternatively-spliced extra domain A of fibronectin promotes acute inflammation and brain injury after cerebral ischemia in mice. Stroke. 2012; 43:1376–82. [PubMed: 22363055]

KHAN MM, YANG WL, BRENNER M, BOLOGNESE AC, WANG P. Cold-inducible RNA-binding protein (CIRP) causes sepsis-associated acute lung injury via induction of endoplasmic reticulum stress. Sci Rep. 2017; 7:41363. [PubMed: 28128330]

KHAN MM, ZAHEER S, THANGAVEL R, PATEL M, KEMPURAJ D, ZAHEER A. Absence of glia maturation factor protects dopaminergic neurons and improves motor behavior in mouse model of parkinsonism. Neurochem Res. 2015; 40:980–90. [PubMed: 25754447]

KIM D, TSAI LH. Linking cell cycle reentry and DNA damage in neurodegeneration. Ann N Y Acad Sci. 2009; 1170:674–9. [PubMed: 19686210]

LAVIN MF, BIRRELL G, CHEN P, KOZLOV S, SCOTT S, GUEVEN N. ATM signaling and genomic stability in response to DNA damage. Mutat Res. 2005; 569:123–32. [PubMed: 15603757]

Author Manuscript Author Manuscript Author Manuscript Author Manuscript

LEDOUX MS, DAUER WT, WARNER TT. Emerging common molecular pathways for primary dystonia. Mov Disord. 2013; 28:968–81. [PubMed: 23893453]

LI Y, WILSON HL, KISS-TOTH E. Regulating STING in health and disease. J Inflamm (Lond). 2017; 14:11. [PubMed: 28596706]

LIPS J, KAINA B. DNA double-strand breaks trigger apoptosis in p53-deficient fibroblasts. Carcinogenesis. 2001; 22:579–85. [PubMed: 11285192]

LIU Q, NIU N, WADA Y, LIU J. The Role of Cdkn1A-Interacting Zinc Finger Protein 1 (CIZ1) in DNA Replication and Pathophysiology. Int J Mol Sci. 2016; 17:212. [PubMed: 26861296]

LIU T, REN X, LI L, YIN L, LIANG K, YU H, REN H, ZHOU W, JING H, KONG C. Ciz1 promotes tumorigenicity of prostate carcinoma cells. Front Biosci (Landmark Ed). 2015; 20:705–15. [PubMed: 25553473]

MARKESBERY WR, LOVELL MA. Damage to lipids, proteins, DNA, and RNA in mild cognitive impairment. Arch Neurol. 2007; 64:954–6. [PubMed: 17620484]

MATTSON MP, CAMANDOLA S. NF-kappaB in neuronal plasticity and neurodegenerative disorders. J Clin Invest. 2001; 107:247–54. [PubMed: 11160145]

MAZZETTI AP, FIORILE MC, PRIMAVERA A, LO BELLO M. Glutathione transferases and neurodegenerative diseases. Neurochem Int. 2015; 82:10–8. [PubMed: 25661512]

MCKAY MJ, BALDWIN JN, FERREIRA P, SIMIC M, VANICEK N, BURNS J. NORMS PROJECT C. Reference values for developing responsive functional outcome measures across the lifespan. Neurology. 2017; 88:1512–1519. [PubMed: 28330961]

MITSUI K, MATSUMOTO A, OHTSUKA S, OHTSUBO M, YOSHIMURA A. Cloning and characterization of a novel p21(Cip1/Waf1)-interacting zinc finger protein, ciz1. Biochem Biophys Res Commun. 1999; 264:457–64. [PubMed: 10529385]

OUCHI Y, YAGI S, YOKOKURA M, SAKAMOTO M. Neuroinflammation in the living brain of Parkinson's disease. Parkinsonism Relat Disord. 2009; 15(Suppl 3):S200–4. [PubMed: 20082990]

PALUDAN SR. Activation and regulation of DNA-driven immune responses. Microbiol Mol Biol Rev. 2015; 79:225–41. [PubMed: 25926682]

PRUDENTE CN, PARDO CA, XIAO J, HANFELT J, HESS EJ, LEDOUX MS, JINNAH HA. Neuropathology of cervical dystonia. Exp Neurol. 2013; 241:95–104. [PubMed: 23195594]

QUEK H, LUFF J, CHEUNG K, KOZLOV S, GATEI M, LEE CS, BELLINGHAM MC, NOAKES PG, LIM YC, BARNETT NL, DINGWALL S, WOLVETANG E, MASHIMO T, ROBERTS TL, LAVIN MF. A rat model of ataxia-telangiectasia: evidence for a neurodegenerative phenotype. Hum Mol Genet. 2017a; 26:109–123. [PubMed: 28007901]

QUEK H, LUFF J, CHEUNG K, KOZLOV S, GATEI M, LEE CS, BELLINGHAM MC, NOAKES PG, LIM YC, BARNETT NL, DINGWALL S, WOLVETANG E, MASHIMO T, ROBERTS TL, LAVIN MF. Rats with a missense mutation in Atm display neuroinflammation and neurodegeneration subsequent to accumulation of cytosolic DNA following unrepaired DNA damage. J Leukoc Biol. 2017b; 101:927–947. [PubMed: 27895165]

RADAK Z, ZHAO Z, GOTO S, KOLTAI E. Age-associated neurodegeneration and oxidative damage to lipids, proteins and DNA. Mol Aspects Med. 2011; 32:305–15. [PubMed: 22020115]

RIDINGS-FIGUEROA R, STEWART ER, NESTEROVA TB, COKER H, PINTACUDA G, GODWIN J, WILSON R, HASLAM A, LILLEY F, RUIGROK R, BAGEGHNI SA, ALBADRANI G, MANSFIELD W, ROULSON JA, BROCKDORFF N, AINSCOUGH JFX, COVERLEY D. The nuclear matrix protein CIZ1 facilitates localization of Xist RNA to the inactive X-chromosome territory. Genes Dev. 2017; 31:876–888. [PubMed: 28546514]

ROGAKOU EP, PILCH DR, ORR AH IV, ANOVA VS, BONNER WM. DNA double-stranded breaks induce histone H2AX phosphorylation on serine 139. J Biol Chem. 1998; 273:5858–68. [PubMed: 9488723]

ROSARIO ER, CARROLL J, PIKE CJ. Testosterone regulation of Alzheimer-like neuropathology in male 3xTg-AD mice involves both estrogen and androgen pathways. Brain Res. 2010; 1359:281–90. [PubMed: 20807511]

ROSS CA, TRUANT R. DNA repair: A unifying mechanism in neurodegeneration. Nature. 2017; 541:34–35. [PubMed: 28002410]

Author Manuscript Author Manuscript Author Manuscript Author Manuscript

SAYKIN AJ, SHEN L, YAO X, KIM S, NHO K, RISACHER SL, RAMANAN VK, FOROUD TM, FABER KM, SARWAR N, MUNSIE LM, HU X, SOARES HD, POTKIN SG, THOMPSON PM, KAUWE JS, KADDURAH-DAOUK R, GREEN RC, TOGA AW, WEINER MW. ALZHEIMER'S DISEASE NEUROIMAGING I. Genetic studies of quantitative MCI and AD phenotypes in ADNI: Progress, opportunities, and plans. Alzheimers Dement. 2015; 11:792–814. [PubMed: 26194313]

SEIDLER RD, BERNARD JA, BURUTOLU TB, FLING BW, GORDON MT, GWIN JT, KWAK Y, LIPPS DB. Motor control and aging: links to age-related brain structural, functional, and biochemical effects. Neurosci Biobehav Rev. 2010; 34:721–33. [PubMed: 19850077]

SEO JE, HASAN M, HAN JS, KANG MJ, JUNG BH, KWOK SK, KIM HY, KWON OS. Experimental autoimmune encephalomyelitis and age-related correlations of NADPH oxidase, MMP-9, and cell adhesion molecules: The increased disease severity and blood-brain barrier permeability in middle-aged mice. J Neuroimmunol. 2015; 287:43–53. [PubMed: 26439961]

SHEN X, CHEN J, LI J, KOFLER J, HERRUP K. Neurons in Vulnerable Regions of the Alzheimer's Disease Brain Display Reduced ATM Signaling. eNeuro. 2016:3.

SILVA AR, SANTOS AC, FARFEL JM, GRINBERG LT, FERRETTI RE, CAMPOS AH, CUNHA IW, BEGNAMI MD, ROCHA RM, CARRARO DM, DE BRAGANCA PEREIRA CA, JACOB-FILHO W, BRENTANI H. Repair of oxidative DNA damage, cell-cycle regulation and neuronal death may influence the clinical manifestation of Alzheimer's disease. PLoS One. 2014; 9:e99897. [PubMed: 24936870]

SOEHNLEIN O, STEFFENS S, HIDALGO A, WEBER C. Neutrophils as protagonists and targets in chronic inflammation. Nat Rev Immunol. 2017; 17:248–261. [PubMed: 28287106]

SUBERBIELLE E, DJUKIC B, EVANS M, KIM DH, TANEJA P, WANG X, FINUCANE M, KNOX J, HO K, DEVIDZE N, MASLIAH E, MUCKE L. DNA repair factor BRCA1 depletion occurs in Alzheimer brains and impairs cognitive function in mice. Nat Commun. 2015; 6:8897. [PubMed: 26615780]

TILSTRA JS, ROBINSON AR, WANG J, GREGG SQ, CLAUSON CL, REAY DP, NASTO LA, ST CROIX CM, USAS A, VO N, HUARD J, CLEMENS PR, STOLZ DB, GUTTRIDGE DC, WATKINS SC, GARINIS GA, WANG Y, NIEDERNHOFER LJ, ROBBINS PD. NF-kappaB inhibition delays DNA damage-induced senescence and aging in mice. J Clin Invest. 2012; 122:2601–12. [PubMed: 22706308]

URYGA A, GRAY K, BENNETT M. DNA Damage and Repair in Vascular Disease. Annu Rev Physiol. 2016; 78:45–66. [PubMed: 26442438]

WARDER DE, KEHERLY MJ. Ciz1, Cip1 interacting zinc finger protein 1 binds the consensus DNA sequence ARYSR(0–2)YYAC. J Biomed Sci. 2003; 10:406–17. [PubMed: 12824700]

XIAO J, UITTI RJ, ZHAO Y, VEMULA SR, PERLMUTTER JS, WSZOLEK ZK, MARAGANORE DM, AUBURGER G, LEUBE B, LEHNHOFF K, LEDOUX MS. Mutations in CIZ1 cause adult onset primary cervical dystonia. Ann Neurol. 2012; 71:458–69. [PubMed: 22447717]

XIAO J, VEMULA SR, XUE Y, KHAN MM, CARLISLE FA, WAITE AJ, BLAKE DJ, DRAGATSIS I, ZHAO Y, LEDOUX MS. Role of major and brain-specific Sgce isoforms in the pathogenesis of myoclonus-dystonia syndrome. Neurobiol Dis. 2017; 98:52–65. [PubMed: 27890709]

XIAO J, VEMULA SR, XUE Y, KHAN MM, KURUVILLA KP, MARQUEZ-LONA EM, COBB MR, LEDOUX MS. Motor phenotypes and molecular networks associated with germline deficiency of Ciz1. Exp Neurol. 2016; 283:110–120. [PubMed: 27163549]

YAN S, SORRELL M, BERMAN Z. Functional interplay between ATM/ATR-mediated DNA damage response and DNA repair pathways in oxidative stress. Cell Mol Life Sci. 2014; 71:3951–67. [PubMed: 24947324]

YATES SC, ZAFAR A, RABAI EM, FOXALL JB, NAGY S, MORRISON KE, CLARKE C, ESIRI MM, CHRISTIE S, SMITH AD, NAGY Z. The effects of two polymorphisms on p21cip1 function and their association with Alzheimer's disease in a population of European descent. PLoS One. 2015; 10:e0114050. [PubMed: 25625488]

YIN J, WANG C, TANG X, SUN H, SHAO Q, YANG X, QU X. CIZ1 regulates the proliferation, cycle distribution and colony formation of RKO human colorectal cancer cells. Mol Med Rep. 2013; 8:1630–4. [PubMed: 24126760]

Author Manuscript Author Manuscript Author Manuscript Author Manuscript

ZENARO E, PIETRONIGRO E, DELLA BIANCA V, PIACENTINO G, MARONGIU L, BUDUI S, TURANO E, ROSSI B, ANGIARI S, DUSI S, MONTRESOR A, CARLUCCI T, NANI S, TOSADORI G, CALCIANO L, CATALUCCI D, BERTON G, BONETTI B, CONSTANTIN G. Neutrophils promote Alzheimer's disease-like pathology and cognitive decline via LFA-1 integrin. Nat Med. 2015; 21:880–6. [PubMed: 26214837]

ZULIANI G, CAVALIERI M, GALVANI M, PASSARO A, MUNARI MR, BOSI C, ZURLO A, FELLIN R. Markers of endothelial dysfunction in older subjects with late onset Alzheimer's disease or vascular dementia. J Neurol Sci. 2008; 272:164–70. [PubMed: 18597785]

Appendix A. Supplementary information

Supplementary information associated with this article can be found, in the online version.

Author Manuscript Author Manuscript Author Manuscript Author Manuscript

Highlights

- Embryonic fibroblasts from *Ciz1* null mice are abnormally sensitive to irradiation
- Aged *Ciz1* null mice exhibit marked deficits in motor and cognitive functioning
- Aged *Ciz1* null mice show increased DNA damage and NF-κB upregulation in brain
- Defects in DNA repair may contribute to global neurological decline in elderly humans

Author Manuscript Author Manuscript Author Manuscript Author Manuscript

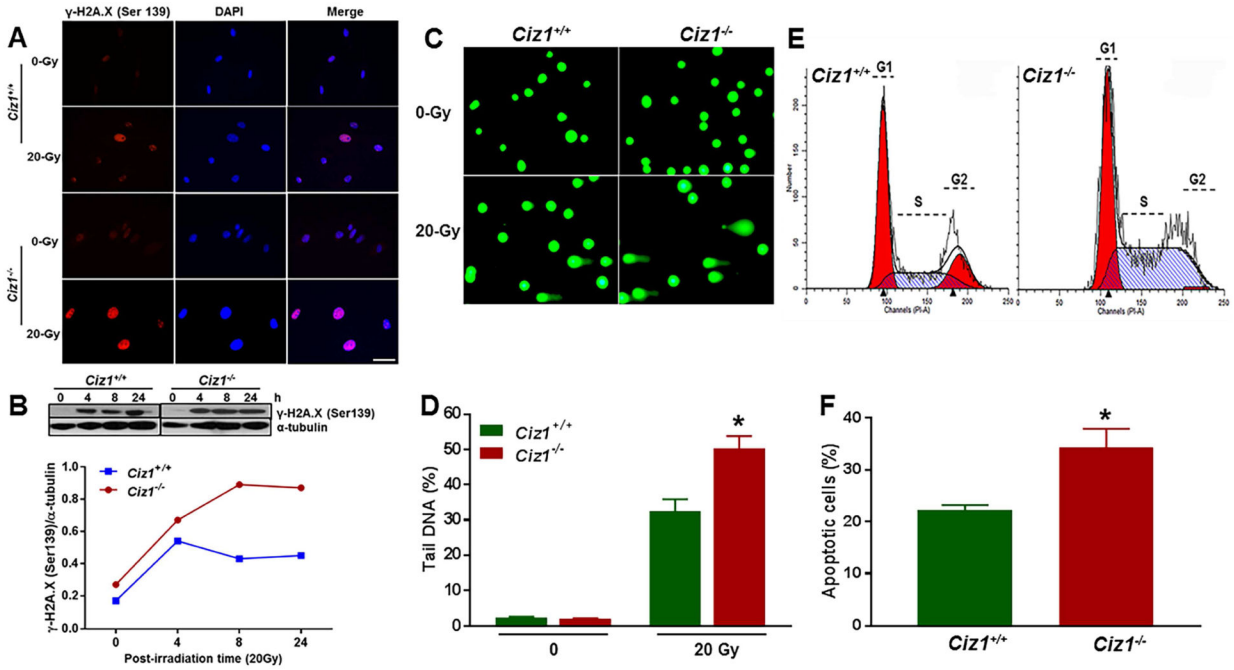

Fig. 1.

CIZ1 deficiency is associated with increased and persistent DSBs, DNA tails, cell-cycle defects and apoptosis in irradiated MEFs. MEFs isolated from *Ciz1*$^{-/-}$ and *Ciz1*$^{+/+}$ embryos were subjected to 20 Gy γ-IR. At 24 h after γ-IR, DNA damage was assessed by γ-H2A.X (ser139) immunohistochemistry (*A*), Western blotting (*B*), comet assays (*C* and *D*) and flow cytometry (*E* and *F*). Untreated MEFs from WT and *Ciz1*$^{-/-}$ mice showed negligible expression of γ-H2A.X (ser139) and largely absent DNA tails. In contrast, *Ciz1*$^{-/-}$ MEFs exposed to γ-IR showed increased γ-H2A.X (ser139) expression along with increased % tail DNA. (*E*) Representative images of flow cytometry analysis of the cell cycle in *Ciz1*$^{+/+}$ and *Ciz1*$^{-/-}$ MEFs. (*F*) In comparison with *Ciz1*$^{+/+}$ MEFs, a higher percentage of *Ciz1*$^{-/-}$ MEFs were apoptotic. Value are expressed as means ± SEM. **P* < 0.05. Scale bar for *A*, 50 μm.

Author Manuscript
Author Manuscript
Author Manuscript
Author Manuscript

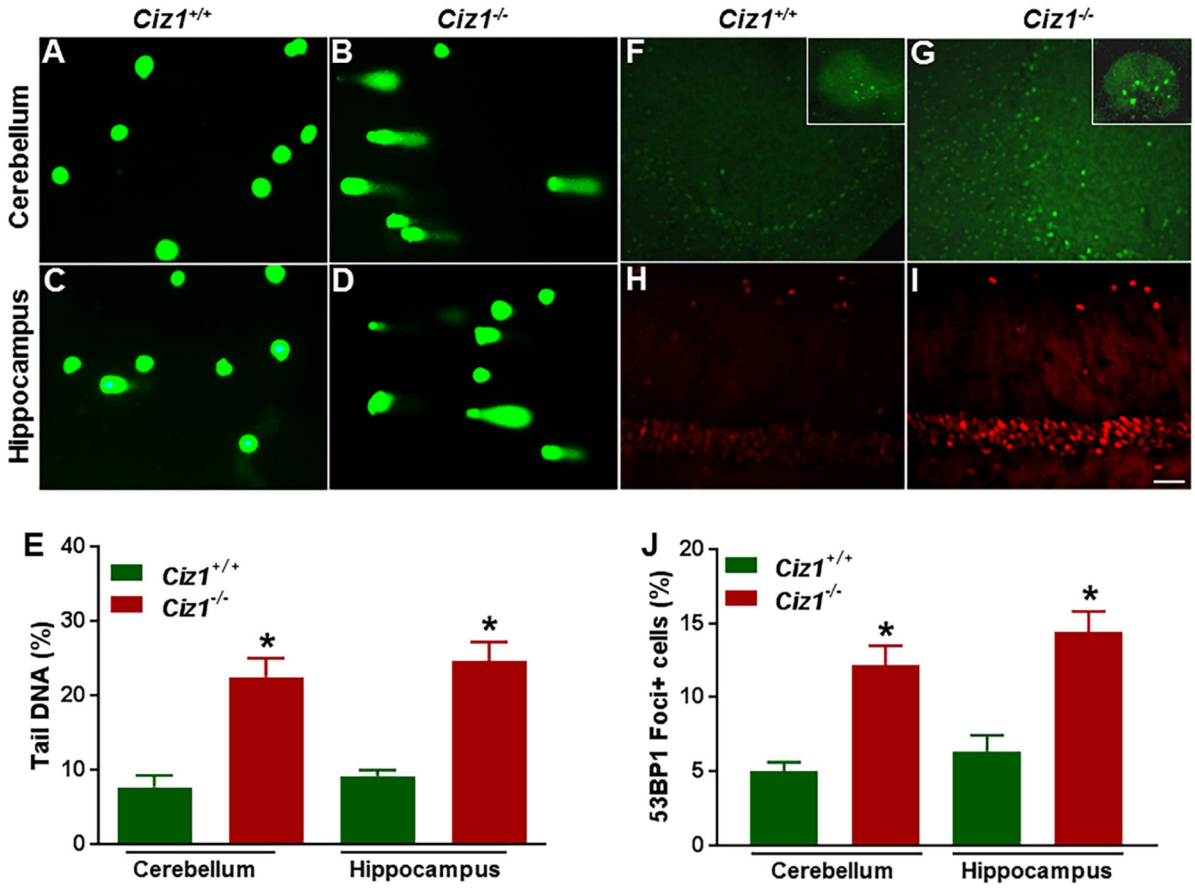

Fig. 2.

CIZ1 deficiency is associated with increased % tail DNA (*A* – *E*) and persistent DSBs (*F* – *J*) in the brains of aged *Ciz1*$^{-/-}$ mice (A–J). Shown are representative images of comet assays [(*A* and *B*; cerebellum) and (*C* and *D*; hippocampus)] and their quantification (*E*). Right-sided panels (*F* – *I*) show 53BP1 immunohistochemistry and its quantification (*J*) in WT and *Ciz1*$^{-/-}$ mice. Value are expressed as means ± SEM. * $P < 0.05$. Scale bar for *F* – *I*, 100 μm.

Author Manuscript Author Manuscript Author Manuscript Author Manuscript

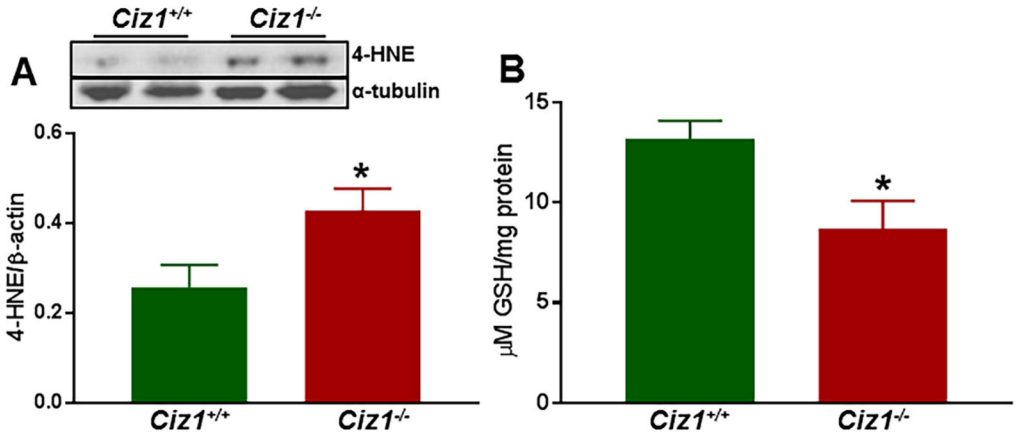

Fig. 3.

CIZ1 deficiency contributes to oxidative stress as measured by lipid peroxidation (4-HNE) and GSH levels in the brains of *Ciz1*$^{-/-}$ mice and WT littermates. Protein levels of 4-HNE (*A*) and GSH (*B*) in brain homogenates were determined by Western blotting and ELISA, respectively. Values are expressed as means ± SEM. **P* < 0.05.

Author Manuscript Author Manuscript Author Manuscript Author Manuscript

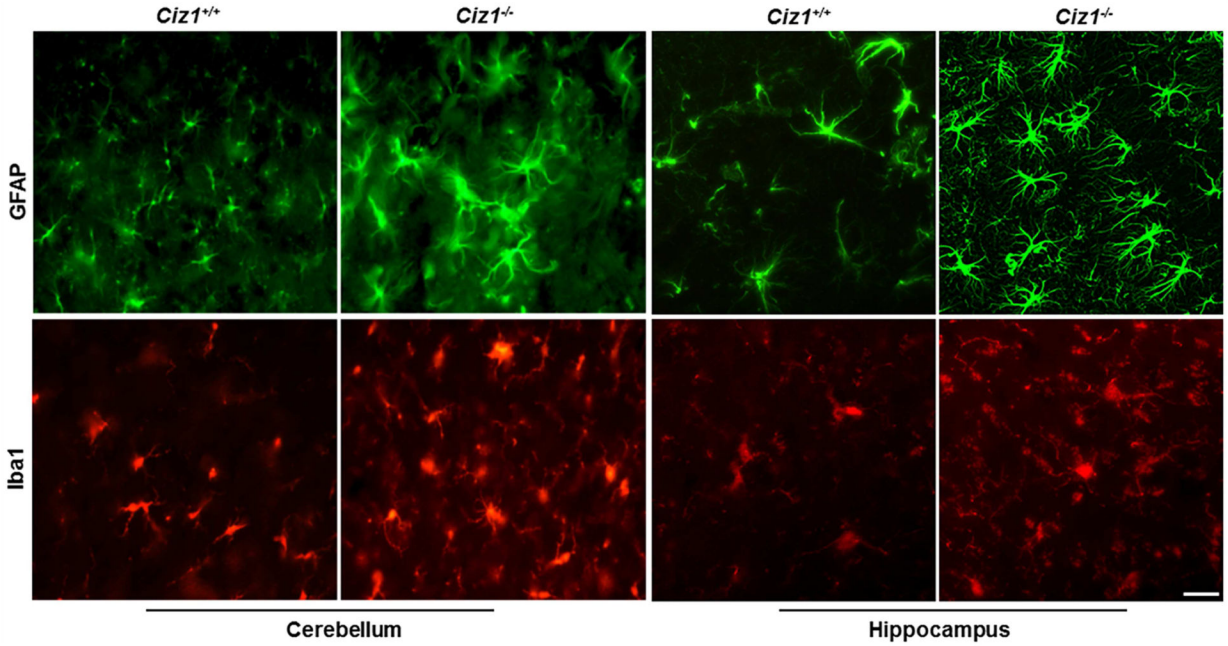

Fig. 4.

Glial activation in the brains of 18-mo-old *Ciz1*$^{-/-}$ mice and *Ciz1*$^{+/+}$ littermates. The expression of microglial (Iba1) and astrocytic (GFAP) markers was determined by immunofluorescence. Marked expression of GFAP (green) and Iba1 (red) positive cells in brain was observed in *Ciz1*$^{-/-}$ mice as compared with *Ciz1*$^{+/+}$ littermates. Scale bar, 20 μm.

Author Manuscript Author Manuscript Author Manuscript Author Manuscript

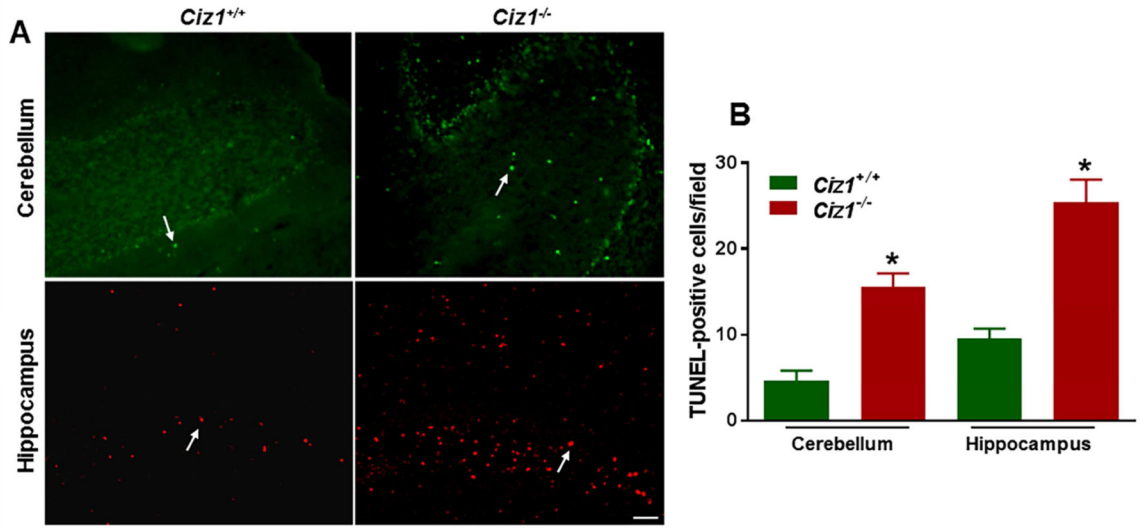

Fig. 5.

CIZ1 deficiency contributes to apoptosis. Brain tissue was harvested from 18-mo-old *Ciz1*$^{-/-}$ mice and WT littermates and processed for TUNEL staining. The left panel shows representative photomicrographs stained for apoptotic cells in cerebellum and hippocampus. The right panel shows quantification of TUNEL-positive cells. In comparison with WT littermates, *Ciz1*$^{-/-}$ mice had a significant increase in the number of apoptotic events. Values are expressed as means ± SEM. **P* < 0.005. Scale bar, 100 μm.

Author Manuscript Author Manuscript Author Manuscript Author Manuscript

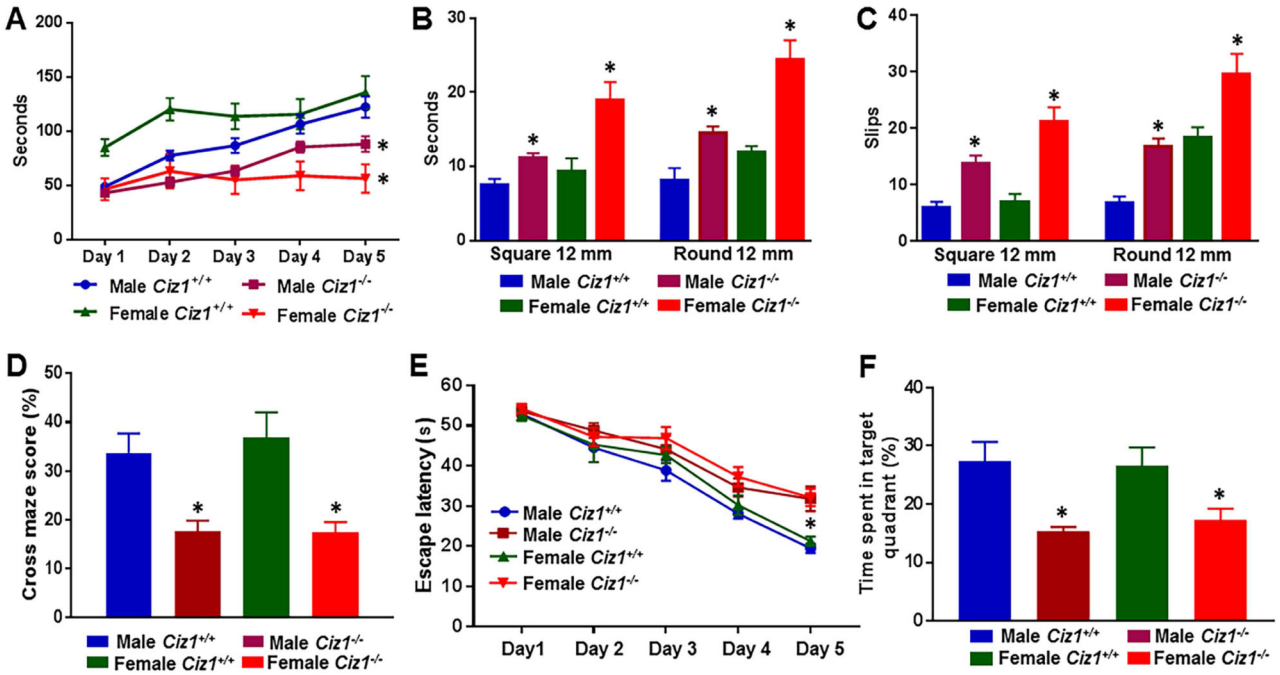

Fig. 6.

Aged *Ciz1*$^{-/-}$ mice and sex-matched WT littermates were analyzed with a battery of behavioral tests (N = 10 – 16/group). (*A*) Rotarod- latency to fall from an accelarating rotating drum was measured. Both male and female *Ciz1*$^{-/-}$ mice had a shorter latency to fall in comparison to WT littermates. (*B* and *C*) Raised beam tasks assessed the ability of mice to traverse narrow beams to reach a dark box. Overall, *Ciz1*$^{-/-}$ mice moved slower and slipped more frequently than WT littermates (*B* and *C,* respectively). (*D*) *Ciz1*$^{-/-}$ mice showed reduced percentages of correct choices in the cross maze task, a measure of working memory. The effect of genotype was promiment in both female and male mice. (*E* and *F*) Morris water maze- aged *Ciz1*$^{-/-}$ mice exhibited decreased escape latencies (*E*) and spent significantly less time in the target quadrant (*F*) when compared to WT littermates. Value are expressed as means ± SEM. *significant effect of genotype within sex ($P < 0.05$).